

# INTEGRATED RADAR INTERFEROMETRY FOR GROUND SUBSIDENCE MONITORING

Linlin Ge<sup>(1)</sup>, Hsing-Chung Chang<sup>(1)</sup>, John Trinder<sup>(1)</sup>, and Chris Rizos<sup>(1)</sup>

<sup>(1)</sup>*School of Surveying & Spatial Information Systems, The University of New South Wales,  
Sydney NSW 2052, AUSTRALIA, Email: l.ge@unsw.edu.au*

## ABSTRACT

This paper reports the progress of the ongoing ESA CAT-1 project (ID 1078). Radar interferometry (InSAR) has been used together with GIS (Geographic Information System) technique to monitor ground subsidence due to underground mining in a test site around the Appin township, southwest of Sydney, Australia. Various digital elevation models (DEMs) are assessed using elevation profiles from ground survey. The best DEM is then employed to remove topographic fringes in the differential InSAR (DInSAR) processing of ERS-1/2 and JERS-1 data. Successful DInSAR results are exported to the GIS and mine subsidence regions extracted. Subsidence profiles derived from the DInSAR results show that JERS-1 repeat-pass DInSAR can achieve +/- 1 cm resolution for subsidence detection while ERS tandem DInSAR can achieve +/- 2 mm in the Australian test site, which highlights the importance and urgency of developing a constellation of InSAR satellites now that high quality DEMs are widely available, so that ground deformation can be monitored with much shorter re-visit time.

## 1 INTRODUCTION

Mine subsidence is movement of the ground surface as a result of the collapse or failure of underground mine workings. In active underground mining operations using longwall mining or high extraction pillar recovery methods, subsidence can occur concurrently with the mining operation in a predictable manner. In abandoned mines where rooms and unmined coal pillars are often left in various sizes and patterns, it may be impossible to predict if and when subsidence will occur. Mine subsidence resulting from abandoned room and pillar mines can generally be classified as either sinkhole subsidence or trough subsidence.

It is a requirement by law in many countries that ground surface subsidence due to underground mining be predicted, monitored and controlled [1][2]. Among the prediction methods, the Incremental Profile Method, which provides site specific mine subsidence predictions thus assisting stakeholders in assessing the potential impacts of underground mining on surface infrastructure, is most commonly used in Australia [3]. Subsidence during the actual mining process is monitored in either 2 dimensions using the levels or total stations or 3 dimensions using GPS on established marks. Measurements from these ground survey have played an important role in improving the models for subsidence predictions. However, since the measurement is done on a point-by-point basis, the spatial coverage of such ground survey is very limited. In order to control the impact of subsidence on major infrastructures (e.g., motorway bridges, tunnels, and telecommunication cables), underground mining is usually stopped well before reaching them, which might be neither necessary nor economic. In order to maximize mining output and better monitor subsidence, the Interferometric Synthetic Aperture Radar (InSAR) has been considered as a complementary technique to the ground survey mentioned above [4][5]. On the other hand, the GIS (Geographic Information System) has been introduced in this paper to assist the quality assessment of digital elevation models (DEMs) and the post-processing of subsidence measurements from InSAR.

The rest of the paper is organized as follows, the second part will discuss the impact of DEM quality on the resolution of 2-pass differential InSAR (DInSAR). Several available DEMs including some derived using data from the ERS Tandem Mission are evaluated against elevation profiles from ground survey. In the third part, the best DEM is used in the repeat-pass DInSAR involving the JERS-1 data in order to find the likely magnitude of mine subsidence as well as the resolution. In the fourth part, the same DEM is employed in the tandem DInSAR involving ERS-1/2 data so that the resolution can be compared to the repeat-pass DInSAR. Note that in this paper 'repeat-pass DInSAR' refers to DInSAR using data from the same satellite and 'tandem DInSAR' is using data from the ERS Tandem Mission as master and slave images in the DInSAR process. In the last part, discussions and concluding remarks are made based on the results.

## 2 DEM QUALITY ASSESSMENT

Photogrammetry has been used together with ground survey to produce DEMs. Fortuitously, recent advancements in techniques for making high-accuracy DEMs such as InSAR and laser scanning may make possible the detection of mine subsidence using space-borne DInSAR and existing satellites. In this section, several DEMs are assessed against ground truth to determine if they are sufficiently accurate to allow for the consistent DInSAR measurement.

InSAR is the study of interference patterns created by combining two sets of radar signals, representing the phase difference ( $d\phi$ ) between the corresponding pixels in the two radar images [6], which can be decomposed into 5 parts, i.e.,

$$d\phi = \phi_{\text{Orbit}} + \phi_{\text{Topo}} + \phi_{\text{Defo}} + \phi_{\text{Atmo}} + \phi_{\text{Noise}} \quad (1)$$

where  $\phi_{\text{Orbit}}$  is the contribution from the inaccurate satellite orbit information;  
 $\phi_{\text{Topo}}$  is the contribution from topography;  
 $\phi_{\text{Defo}}$  is the contribution from ground surface movement / deformation;  
 $\phi_{\text{Atmo}}$  is the contribution from atmosphere; and  
 $\phi_{\text{Noise}}$  is radar noise.

From Eq (1) it can be seen that by removing the orbit contribution, InSAR has the ability to measure the actual elevation of the Earth's surface (assuming that deformation between two radar acquisitions and other contributors can be neglected, as in the case of single-pass InSAR or the ERS Tandem Mission). As a matter of fact, most of an InSAR phase signal arises from parallax viewing from two radar antenna locations (from two orbital passes in the repeat pass method), with perpendicular baseline typically separated by 0 to 1000 m. This parallax results in phase differences that correspond to surface topography, similar to stereo pairs of air photos. Thus, InSAR is a powerful tool for making DEMs.

Differential InSAR, on the other hand, has the ability to measure small changes in elevation of the Earth's surface once the actual elevations ( $\phi_{\text{Topo}}$ ) are accounted for. Surface deformations also contribute to InSAR phase since they contribute to path-length changes, independent of the baseline. These two contributors, static topography ( $\phi_{\text{Topo}}$ ) and surface deformation ( $\phi_{\text{Defo}}$ ), are separated using differential InSAR where two interferograms are subtracted from one another, one of which is a synthetic interferogram made from a DEM that contains only static topographic information (i.e., no deformation). Deformation due to earthquakes, surface subsidence due to well-pumping, volcanic inflation, and glacier motion are some well-known examples of DInSAR accomplishments to date. The clarity of this deformation signal is therefore dependent on the accuracy with which we eliminate the topography; that is, errors in modeling the topography will introduce residual noise into the deformation signal. This uncertainty in topography can introduce a noise floor above the subsidence signal level, especially with shorter-wavelength sensors that have less signal strength. Therefore, DEM accuracy plays a key role in increasing the DInSAR signal-to-noise ratio and thus the resolution.

When small baselines are used, the influence of topography is small and the quality of the DEM used for the synthetic interferogram is less important. Unfortunately, baselines vary over a wide range in the space-borne case, meaning that many pairs of data go unused because baselines are too large due to spatial decorrelation. Traditionally, DEM errors have restricted results to the detection of signals on the order of a centimeter or more; but recent, more accurate DEMs can reduce topographic noise to the point where millimeter-scale change detection may be possible with substantially relaxed spatial baseline requirements, increasing the number of useful pairs of radar acquisitions.

A mathematical description for the influence of elevation uncertainty on DInSAR resolution can be found from basic SAR theory. Topographic phase is dependent on the baseline separation between the satellite's positions at the times of acquisition (Eq (2)), whereas the deformation phase does not have this dependency (Eq (3)) [6],

$$\phi_{\text{Topo}} = (h \cdot 2k \cdot B_n) / (R \cdot \sin \alpha) \quad (2)$$

$$\phi_{\text{Defo}} = \delta \cdot 2k \quad (3)$$

where  $\phi_{\text{Topo}}$  is topographic phase;  
 $h$  is topographic height in meters;

$k$  is the wavenumber (i.e.  $2\pi/\lambda$ ,  $\lambda$  is the wavelength of radar);  
 $B_n$  is the perpendicular baseline separation between two satellite passes;  
 $R$  is sensor height above ground;  
 $\alpha$  is the incidence angle;  
 $\varphi_{\text{Defo}}$  is deformation phase; and  
 $\delta$  is change in path length in meters in the line-of-sight direction.

For the purposes here, assuming that  $k$ ,  $B_n$ ,  $R$ , and  $\alpha$  are sufficiently well known to not introduce noticeable noise, leaving  $h$  as the primary uncertainty in Eq (2), and  $\delta$  as the signal of interest. If we assume that a signal-to-noise ratio of 0 dB is the minimum required to ensure valid interpretations, then equating  $\varphi_{\text{Topo}}$  to  $\varphi_{\text{Defo}}$  yields an equation for  $\delta$  versus  $h$  that can be parameterized by  $B_n$  as shown graphically in Fig 1. Note that the unit of horizontal axis is mm.

### Relationship between DEM Vertical Accuracy and Phase-signal Strength

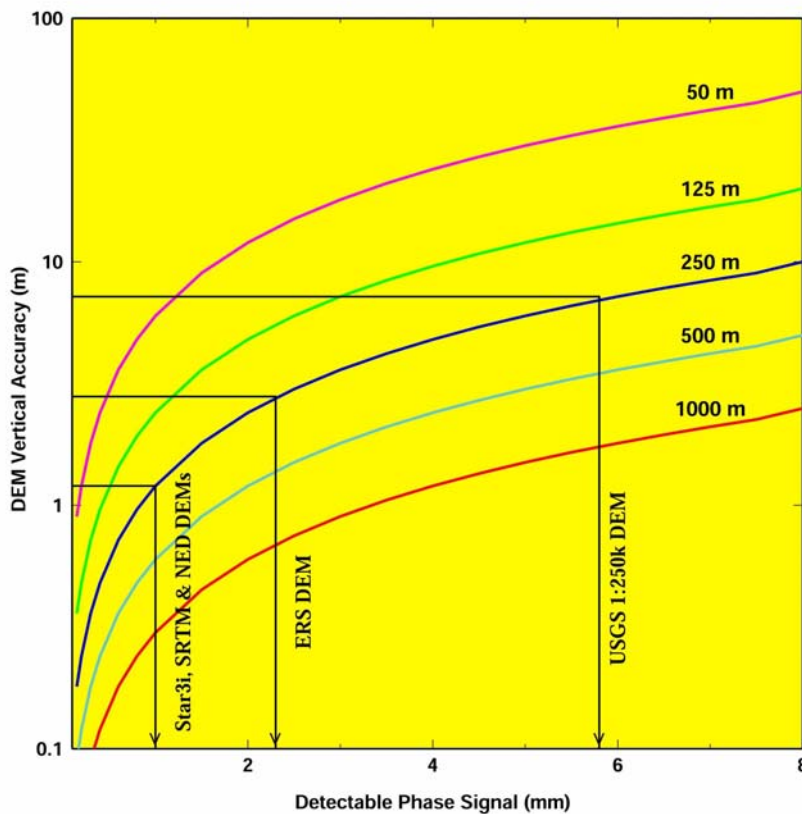


Figure 1 Detectable subsidence signal versus DEM vertical accuracy parameterized by perpendicular baseline.

Figure 1 shows required DEM accuracies for five typical baselines. If the perpendicular baseline is known, Fig 1 can be used to determine the DEM accuracy required to be able to measure a certain signal reliably. Given a perpendicular baseline of 250 m, for example, the detectable signal level gets smaller and smaller as the quality of the DEM improves from the USGS 1:250,000, to one created from ERS-2 data, to the higher-quality DEMs at the far left. Or given an uncertainty in topographic accuracy, Figure 1 can be used to determine the maximum allowable baseline required to measure particular signal amplitude. Such information may also be useful when determining whether a particular interferometric pair (separated by 24, 35 or 44 days for Radarsat, ERS-1/2 or JERS-1, respectively) is worth purchasing or analyzing, given a signal-level of interest.

As DEM accuracy improves, therefore, several new DInSAR applications may now become possible. While Earth deformation rates of several millimeters per year in some parts of the world have been measured using GPS, typically these must be measured by InSAR over time intervals long enough for the deformation to be a centimeter or more.

These long time intervals increase the chances of temporal de-correlation, decrease the number of usable InSAR pairs, and eliminate the possibility of measuring intermediate fluctuations in deformation rates. Hence, it is a much better option to monitor deformation with satellites of shorter re-visit time employing a highly accurate DEM. This will be demonstrated in the following two sections.

Before moving on to DInSAR in the next two sections, seven DEMs (including some generated from the ERS Tandem data) available to the test sites of Appin and West Cliff, both southwest of Sydney, Australia, are assessed against ground truth. All the DEMs are imported to the GIS and so are the ground survey data. They are then carefully geo-referenced. Elevation profiles are derived from these DEMs along the ground survey line (ground truth elevation represented as “DEM A” in red) in Appin as shown in Fig 2. For clarity, 4 DEM profiles are plotted in the upper part (“DEM F, E, H, and G”) and 3 in the lower part (“DEM D, C, and B”). By visual inspection, it can be seen that “DEM F” is the closest to the ground truth on the Appin line.

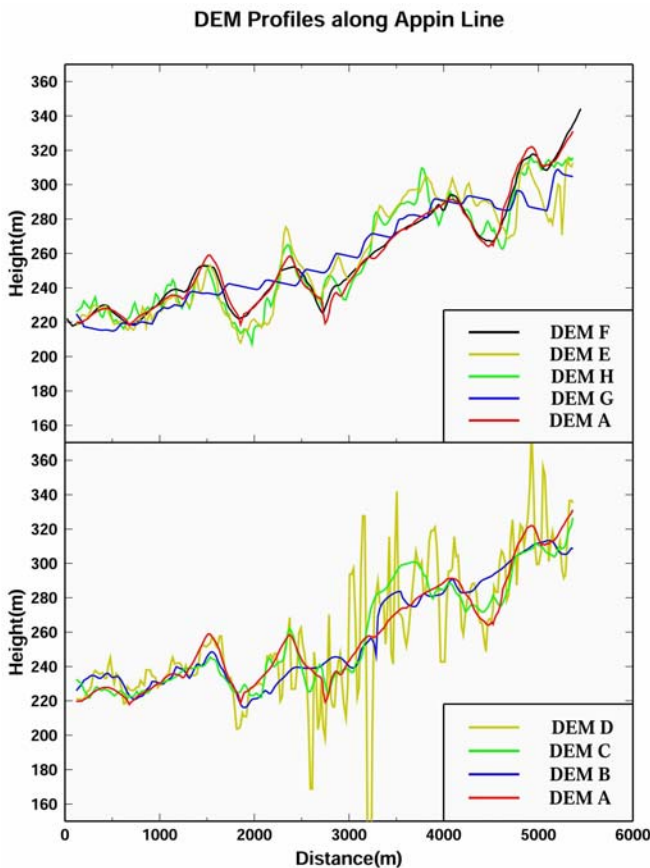


Figure 2 DEM quality assessment using ground truth.

The DEMs are also compared to other three ground survey lines in West Cliff in a similar way. Table 1 summarizes the RMS (root-mean-square) errors of the seven DEMs against the ground truth on the Appin line as well as other three lines in the West Cliff. The first row indicates the difference of maximum and minimum elevations (terrain changes) on the ground survey lines. From the table it can also be concluded that “DEM F” is the best one which gives a DEM of 20 m posting and 5 m RMS vertical accuracy. In the following two sections, this DEM is employed in the DInSAR processing.

Table 1 RMS errors of the seven DEMs against ground truth.

		Appin	West Cliff		
			A	B	C
Max - Min		127.45	37.32	67.01	77.17
RMS (m)	DEM E	10.46	6.23	12.46	5.92
	DEM H	9.63	5.38	7.93	6.85
	DEM G	14.34	7.48	9.15	10.74
	DEM C	9.61	10.50	10.30	9.47
	DEM D	27.88	12.88	14.14	15.23
	DEM B	14.07	7.72	15.44	6.22
	DEM F	3.14	3.59	3.10	4.38

### 3 MINE SUBSIDENCE MAPPED BY REPEAT-PASS DIFFERENTIAL INSAR

As mentioned in section 1, in order for DInSAR to measure ground deformation the time intervals between the master and slave SAR acquisitions normally has to be long enough for the deformation to be a centimeter or more. Therefore, a repeat-pass pair acquired by the JERS-1 satellite (master: 21 April 1995; slave: 4 June 1995; temporal baseline: 44 days; perpendicular baseline: 482m) is analyzed first. Considering this baseline and the DEM of 5 m height accuracy used, the resolvable subsidence signal should be around 5 mm according to Fig 1. Fig 3 gives the DInSAR result after post-processing in the GIS. The yellow lines are the ground survey routes and the red panels are the underground mining longwalls. The subsidence region is represented in color and the color bars at right show the amount of subsidence. It can be seen that the maximum subsidence in this case is almost 25 cm. Also evident is the much better coverage of InSAR over the ground survey – although 4 ground survey lines have been set up only Line D touched the subsiding region a bit. The subsidence detected by the ground survey on this line would be 2-4 cm which is certainly NOT representative.

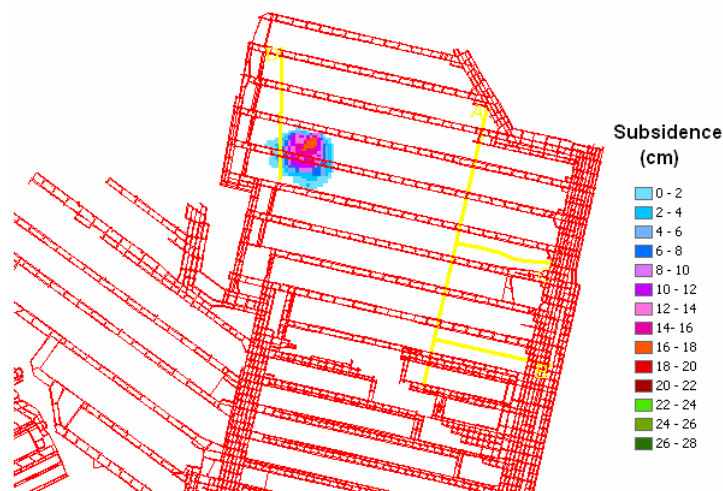


Figure 3 Subsidence detected by DInSAR overlaid on the mine plan (21 April 1995 and 4 June 1995 JERS-1 pair).

Profiles of subsidence passing through the maximum subsiding point have been derived from the DInSAR result in order to analyse its resolution on subsidence (Figure 4). The central part is the subsiding region while on the left- and right-hand sides the stable regions. *The variations in the stable regions indicate that the resolution of DInSAR is about +/- 1 cm.* Figure 5 gives another subsidence profile also demonstrating +/- 1 cm resolution of DInSAR.

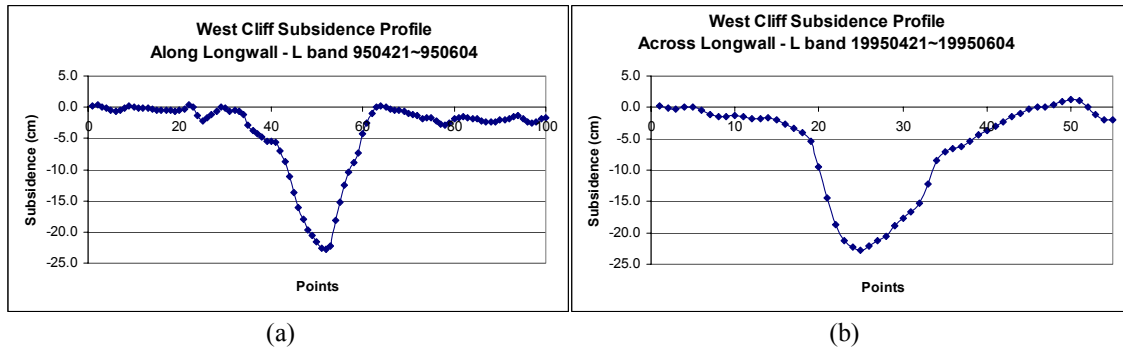


Figure 4 Subsidence profiles along (a) and across (b) the longwall (21 April 1995 and 4 June 1995 JERS-1 pair).

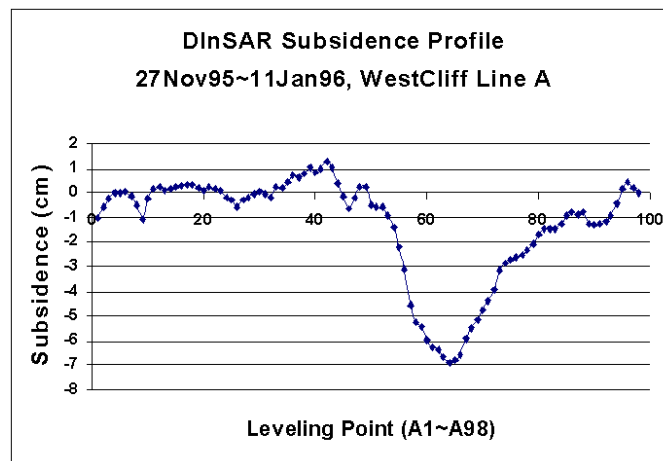
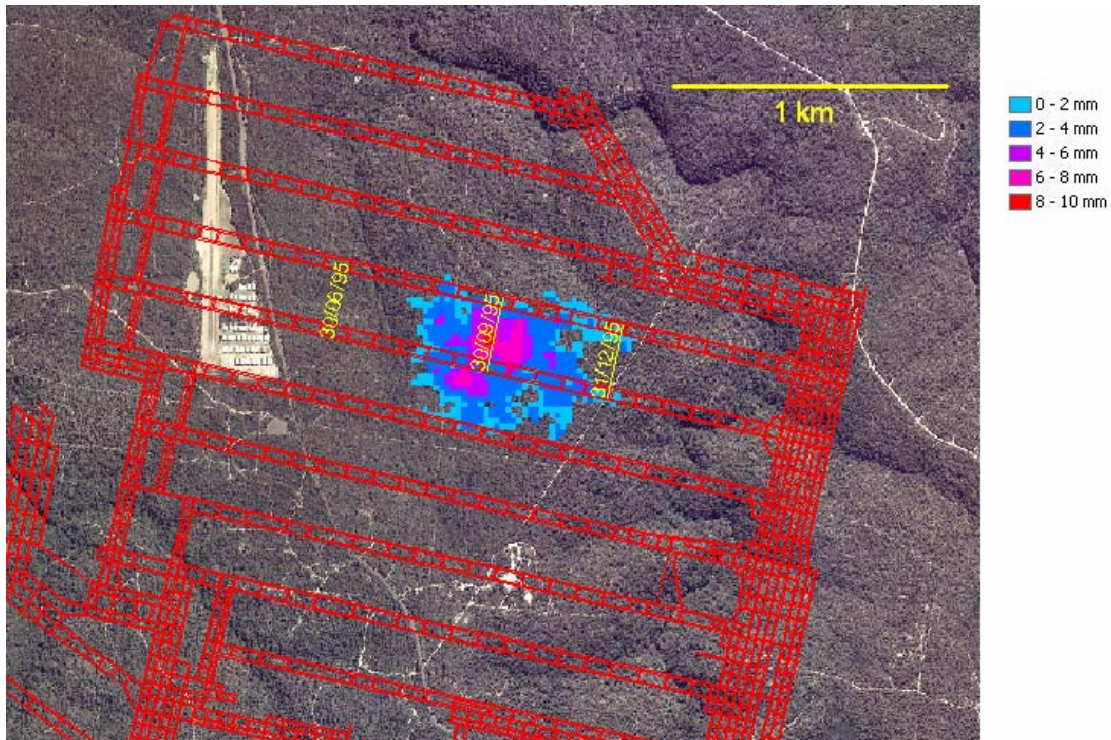


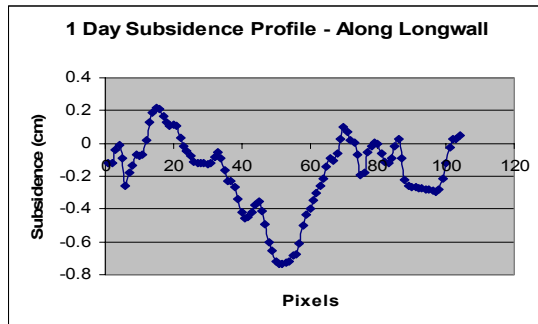
Figure 5 Subsidence profiles derived along the West Cliff Line A (27 November 1995 and 11 January 1996 JERS-1 pair).

#### 4 MINE SUBSIDENCE MAPPED BY ERS TANDEM DIFFERENTIAL INSAR

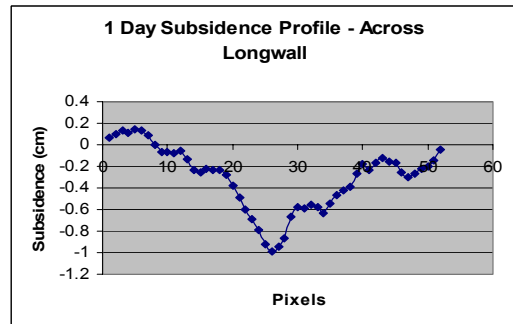
Although in the previous section the maximum subsidence in West Cliff detected by repeat-pass DInSAR is about 25 cm over a period of 44 days (0.6 cm / day on the average), it is still quite likely that the amount of subsidence in one day can be as much as 1 cm since mine subsidence is a non-linear process and most of it happens immediately after mining. Therefore, it makes sense to try DInSAR on the ERS tandem data. The available ERS tandem pair (master: 29 October 1995; slave: 30 October 1995; temporal baseline: 24 hours; perpendicular baseline: -49m) is analyzed. Considering this baseline and the DEM of 5 m height accuracy used, the resolvable subsidence signal should be better than 1 mm according to Fig 1. Fig 6 gives the DInSAR result after post-processing in the GIS. Mining progress from underground survey is also plotted on the panel. *It can be seen that the maximum subsidence in 24 hours is 1 cm and the tandem DInSAR resolution is +/- 2 mm.* It is amazing that mine subsidence has been mapped with such subtle detail. Therefore, the tandem DInSAR resolution has been improved by the order of almost one magnitude over the repeat-pass DInSAR, again highlighting the importance of developing a constellation of InSAR satellites so that ground deformation can be monitored with much shorter re-visit time[7][8].



(a)



(b)



(c)

Figure 6 Subsidence detected by DInSAR overlaid on the aerial photo and mine plan (ERS tandem pair 29/30 October 1995) (a) and subsidence profiles along (b) and across (c) the longwall.

## 5 CONCLUDING REMARKS

The progress of the ongoing ESA CAT-1 project (ID 1078) has been reported. By integrating InSAR and GIS technologies, mine subsidence has been detected at +/- 1 cm resolution using the JERS-1 repeat-pass DInSAR and at +/- 2 mm resolution using ERS tandem DInSAR in the Australian test site. The integrated technique has been demonstrated operational for monitoring mine subsidence. The research also highlights the importance and urgency of developing a constellation of InSAR satellites now that high quality DEMs are widely available, so that ground deformation can be monitored with much shorter re-visit time.

## ACKNOWLEDGMENT

The authors wish to thank A/Prof Makoto Omura of Kochi Women's University, Japan, for providing L-band data, and Mr Craig Smith of ACRES (the Australian Centre for Remote Sensing) for providing C-band SAR images. Both the Australian Research Council and the Australian Coal Association Research Program are acknowledged for funding the research.

## REFERENCES

1. Mine Subsidence Compensation Act , Australia, 1961.
2. Federal Mine Safety & Health Act of 1977, Public Law 91-173, USA, 1977.
3. Waddington Kay & Associates, <http://www.minesubsidence.com/>, 2003.
4. Spreckels, V., et al, Detection and observation of underground coal mining-induced surface deformation with differential SAR interferometry, Proc. Joint Workshop of ISPRS Working Groups I/2, I/5 and IV/7: "High Resolution Mapping From Space", 227-234, Hannover, Germany, Sept. 19-21, 2001.
5. Ge, L., X. Li, and C. Rizos, GPS and GIS Assisted radar interferometry. Advanced International Workshop on InSAR for Measuring Topography and Deformation of the Earth Surface, Hong Kong , December 16-17, 2002.
6. Massonnet, D., and K. Feigl, Radar interferometry and its application to changes in the Earth's surface, Reviews of Geophysics, 36, 441–500, 1998.
7. Solomon, S.C., et al, Plan for Living on a Restless Planet Sets NASA's Solid Earth Agenda, EOS Transactions, American Geophysical Union, Vol. 84, No. 45, P485&491, 2003.
8. China to build satellite group in space, [http://www1.chinadaily.com.cn/en/doc/2003-11/10/content\\_280275.htm](http://www1.chinadaily.com.cn/en/doc/2003-11/10/content_280275.htm), 2003.